

Hall Effect and Resistivity Study of the Magnetic Transition, Carrier Content, and Fermi-Liquid Behavior in $\text{Ba}(\text{Fe}_{1-x}\text{Co}_x)_2\text{As}_2$

F. Rullier-Albenque,^{1,*} D. Colson,¹ A. Forget,¹ and H. Alloul²

¹*Service de Physique de l'Etat Condensé, Orme des Merisiers, CEA Saclay (CNRS URA 2464), 91191 Gif sur Yvette cedex, France*

²*Laboratoire de Physique des Solides, UMR CNRS 8502, Université Paris Sud, 91405 Orsay, France*

(Received 30 March 2009; published 30 July 2009)

The negative Hall constant R_H measured all over the phase diagram of $\text{Ba}(\text{Fe}_{1-x}\text{Co}_x)_2\text{As}_2$ allows us to show that electron carriers always dominate the transport properties. The evolution of R_H with x at low doping ($x < 2\%$) indicates that important band structure changes happen for $x < 2\%$ prior to the emergence of superconductivity. For higher x , a change with T of the electron concentration is required to explain the low T variations of R_H , while the electron scattering rate displays the T^2 law expected for a Fermi liquid. The $T = 0$ residual scattering is affected by Co disorder in the magnetic phase, but is rather dominated by incipient disorder in the paramagnetic state.

DOI: 10.1103/PhysRevLett.103.057001

PACS numbers: 74.70.Dd, 72.15.Lh, 74.25.Dw, 74.25.Fy

Introduction.—Despite the similarity of phase diagrams of cuprates and iron based pnictides [1–3], it is already well established that the underlying physics of these compounds is different. While cuprates are doped Mott insulators with properties tightly related to the effects of strong electron correlations in the narrow Cu $3d$ band, iron pnictides are metallic systems with a spin density wave (SDW) state at low doping. They display a semimetal band structure with three hole bands and two electron bands close to the Fermi level E_F as obtained by electronic structure calculations [4–6] and confirmed by angular resolved photoemission spectroscopy (ARPES) [7,8]. The SDW ordering is often attributed to the nesting between electron and hole cylindrical bands. The interband interaction between the quasi nested bands could be as well at the origin of the high- T_c values [9]. The proximity and/or coexistence of antiferromagnetism and superconductivity (SC) in the Fe-pnictides and the detection of spin fluctuations by NMR [10] have been also taken as an indication that magnetic fluctuations may play a decisive role in the SC pairing mechanism as proposed for the high- T_c cuprates.

Surprisingly, although some linear dependences of resistivity have been taken as indications for a quantum critical point [11], systematic analyses of the transport properties to reveal features expected for such a band structure have not been performed so far all over the phase diagram. Presently such studies appear accessible for the $\text{Ba}(\text{Fe}_{1-x}\text{Co}_x)_2\text{As}_2$ family as fine tuning of Co content can be achieved in sizeable single crystals, allowing then to span the entire electron doped phase diagram [3,12–15]. Investigations of the influence of Co disorder in Fe layers are still missing, even if it has been pointed out [12] that Co substitution has less incidence on SC than in plane substitutions in the cuprates [16]. We address these points in this work by performing extensive measurements of resistivity ρ and Hall coefficient R_H , similar to those reported simultaneously in [17]. Here the great accuracy of our data allows us to demonstrate that the hole contribution to the

transport can be neglected at low T in most of the phase diagram. This leads us to propose that in this pnictide family the electron carriers have archetypal Fermi liquid behavior, with large T^2 contributions to the electron scattering rate, as $k_B T$ can become sizeable with respect to E_F . The hole contribution to the transport is found anomalous and only perceptible at high T for low x . At the magnetic transition T_{SDW} of the undoped parent compound, R_H is found to evolve in two steps which appear to correspond to the successive gapping of the electronic bands with decreasing T .

Samples and resistivity measurements.—Single crystals of $\text{Ba}(\text{Fe}_{1-x}\text{Co}_x)_2\text{As}_2$ with Co contents x ranging from 0 to 0.2 were grown using the self-flux method [18]. Starting reagents of high purity Ba, FeAs, and CoAs were mixed in the molar ratio 1 : (4 - x) : x , loaded in alumina crucibles, and then sealed in evacuated quartz tubes. The mixture was typically held at 1180 °C for 4 hours, slowly cooled down to 1000 °C/h at 5 °C/h, then down to room temperature at 200 °C/h. Single crystals could be extracted mechanically from the solid flux. Chemical analyses were performed with an electron probe (Camebax 50), on several crystals for each Co doping, yielding the Co content within 0.5% absolute accuracy. In-plane resistivity measurements using either the standard dc four-probe or the van der Pauw technique [19] were performed on samples which have been cleaved from larger crystals to thicknesses lower than 30 μm . Two or three different samples were measured for each Co doping, and a good reproducibility of the data was found both for the T dependence of ρ and its absolute values (better than 10% accuracy, whatever the technique used).

The qualitative features of our $\rho(T)$ data displayed in Fig. 1 on a series of samples match reported results [3,12,14]: the drop of resistivity at 135 K, which signals the structural and SDW transitions in the undoped parent, is replaced by a steplike increase of $\rho(T)$ as soon as Co is inserted. Upon Co doping, this transition is shifted to lower

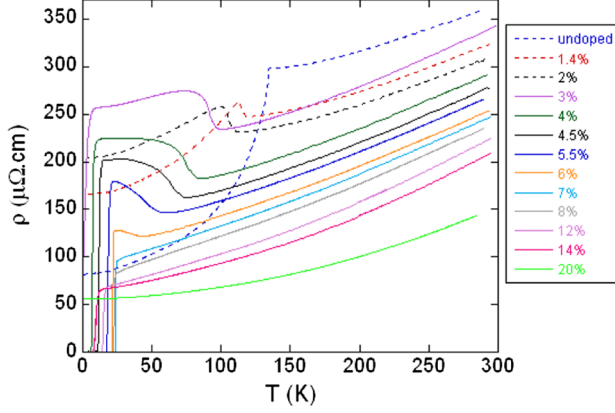


FIG. 1 (color online). Temperature dependence of the in-plane resistivity $\rho(T)$ of $\text{Ba}(\text{Fe}_{1-x}\text{Co}_x)_2\text{As}_2$ single crystals. For the sake of clarity, the data for the undoped parent and low doped non SC samples, which evolve differently than for higher Co content, are plotted with dashed lines. Notice the singularities associated with the SDW transitions.

T and SC is observed within the doping range $0.03 \leq x \leq 0.15$, showing the coexistence of SC and SDW order for $0.03 \leq x \leq 0.07$. We notice that a marked change in the evolution of $\rho(T)$ curves occurs at about $x = 0.03$ for which SC appears. In both the paramagnetic and SDW phases, ρ only starts there to decrease monotonously with Co content. Another puzzling observation concerns the T dependences of ρ in the paramagnetic phase which parallel each other for most Co dopings. This seems difficult to conciliate with a multiband description of the electronic structure for which the conductivity σ is the sum of the hole and electron contributions ($\sigma = 1/\rho = \sigma_e + \sigma_h$). How could the evolutions with x of the concentrations and relative mobilities of the two types of carriers compensate and give similar T dependent contributions to ρ whatever x ?

Hall effect.—In order to get more insight into the evolution of transport properties, we have then performed Hall effect measurements on the same samples, and checked the linearity in H of the Hall voltage up 8 T in the paramagnetic phase. The data for the Hall coefficient R_H are presented in the inset of Fig. 2 for a set of Co dopings. The strong increases in the magnitude of R_H at the SDW transitions will be discussed later. In order to better visualize the behavior of R_H in the paramagnetic phases and for large x , we have plotted in Fig. 2 the variations of the Hall number $n_H = 1/(eR_H)$. Assuming a simple two band model, one could write

$$eR_H = \frac{1}{n_H} = \frac{\sigma_h^2}{n_h(\sigma_e + \sigma_h)^2} - \frac{\sigma_e^2}{n_e(\sigma_e + \sigma_h)^2} \quad (1)$$

where n_e (n_h) are the concentration of electrons (holes) usually taken as T independent in a metallic state. One should note that charge conservation implies

$$n_e = n_h + x, \quad (2)$$

with the usual assumption that Co gives an electron to these

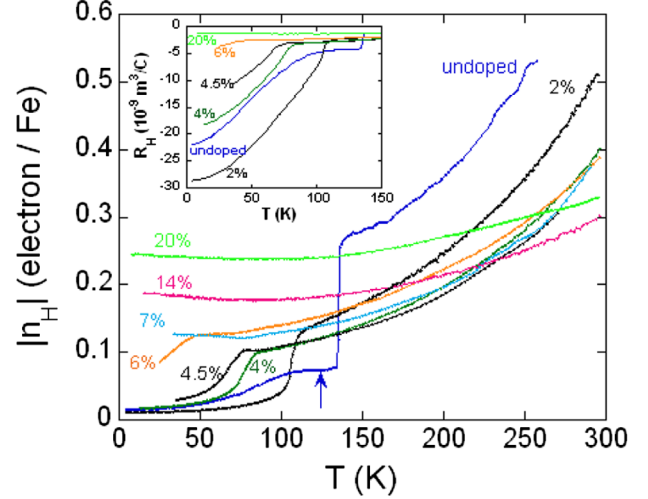


FIG. 2 (color online). T variation of the Hall number $|n_H|$ for a selected set of samples. Here, n_H (e/Fe) = $0.32 \times 10^{-9}/R_H$ (m^3/C). For the undoped compound, the drop below T_{SDW} occurs in two steps, the value on the plateau indicated by an arrow being $0.074 e/\text{Fe}$. Inset: Raw data for the magnetic samples showing the drops of R_H at T_{SDW} . The data for the most overdoped sample have been kept for comparison.

bands. As we have only three relations for n_e , n_h , σ_e , σ_h , the problem cannot be readily solved without further elements based on physical arguments or other experiments. However, the negative sign of R_H indicates that electrons give the dominant contribution to the charge transport at all T whatever x with the value of n_H being an upper limit for the electron concentration n_e .

For large Co doping, ARPES experiments show that the hole Fermi surface pockets become very small while the electron pockets significantly expand [20]. In this case, $n_h \ll n_e$ (and $\sigma_h \ll \sigma_e$) so that Eq. (1) writes

$$|n_H| \approx n_e(1 + 2\sigma_h/\sigma) \quad (3)$$

to first order in σ_h/σ . This simple limit permits us to evidence that, whatever the exact value of n_e , the data for $\rho(T)$ and $|n_H(T)|$ would only be explained by a high T increase of σ_h with a weak minimum below 100 K. This behavior, opposite to that expected for a metallic system, leads us to conclude that n_e and n_h are T dependent.

For the most doped samples for which hole contributions to both $n_H(T)$ and $\rho(T)$ can be neglected, these quantities resume then into the single band expressions,

$$n_H(T) = n_e(T) \quad \text{and} \quad \rho(T) = \frac{m_e}{n_e(T)e^2\tau(T)}, \quad (4)$$

where m_e is the electron effective mass. The limiting values of n_e at $T = 0$ deduced from the low T data for $|n_H|$ are plotted in Fig. 3 versus Co content. In this plot, we have reported as well the data for the magnetic samples for which $|n_H|$ flattens out just above T_{SDW} . We find that $|n_H(T = 0)|$ increases linearly with x which supports the idea that the low T value of $|n_H|$ can be assimilated to the

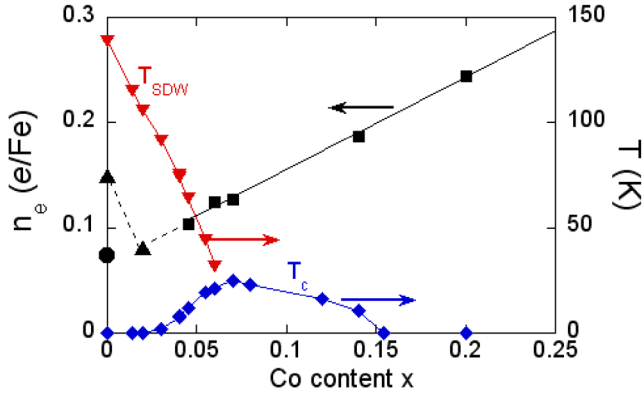


FIG. 3 (color online). Phase diagram of $\text{Ba}(\text{Fe}_{1-x}\text{Co}_x)_2\text{As}_2$ where T_{SDW} (\blacktriangledown) has been taken at the minimum of $d\rho/dT$ [27]. (\blacksquare): values of n_e determined at low T for $x \geq 4\%$. The linear fit (full line) extrapolates for $x=0$ to 0.07, close to the value (\bullet) of the intermediate plateau of $|n_H(T)|$ (arrow in Fig. 2). Extrapolations from the paramagnetic phase (\blacktriangle), assuming T^2 variations for $n_H(T)$ as found for higher x , allow us to conjecture the evolution of n_e (dash line) which would take place below $x = 0.03$ in the absence of magnetic ordering.

actual value of n_e down to $x \approx 4\%$. Each Co adds ~ 0.9 e/Fe and only reduces n_h from 0.06 to 0.04 hole/Fe for $0.04 \leq x \leq 0.2$. In the simple rigid band model, this trend can be expected, as the shift of E_F yields different changes of n_e and n_h if shapes of the pockets (and/or effective masses) are different for the two types of carriers, as evidenced by ARPES [8,20].

As for the small T variation of the carrier content for $T \leq 150$ K, it can be assigned to the fact that E_F is only 20–40 meV above the bottom of the electron bands in the BaFe_2As_2 family as shown by ARPES [8,21]. Thermal population of the hole and electron bands yields then a shift of the chemical potential $\mu(T)$ to fulfill Eq. (2). However, this band effect might not be sufficient to explain the huge increase of n_H by a factor 3 to 5 observed above 150 K for $x \leq 7\%$. Here, we might consider that the smallness of σ_h at low T could result from the localization of holes in low energy states (such as defects). The T variations of μ and of the carrier contents would then result from the high T release of such states.

Electron scattering rate.—So far we have interpreted satisfactorily the low T Hall data assuming that the holes do not contribute to the charge transport. The quantity $\cot(\Theta_H) = \rho/|R_H|$ equals $m_e/e\tau$ in the single band case of Eqs. (4), and gives a direct determination of the electron scattering rate $1/\tau(T)$ when this limit applies. We have then reported in Fig. 4(a) the data for $\cot(\Theta_H)$ for all our superconducting samples. The very similar behavior displayed by $\cot(\Theta_H)$ for all x does not show up any *direct* incidence on the transport of the spin fluctuations detected above T_{SDW} in the nuclear spin lattice relaxation rates [10]. This might lead us to anticipate that the variation of n_H is always governed by a T variation of n_e , even for the lower

Co contents. As shown in Fig. 4(b) for $x > 4\%$, this yields $1/\tau(T)$ data which split, as usual, in a T -dependent $1/\tau_e(T)$ and a residual $1/\tau_0$. The former is very well fitted below 150 K by a Fermi-liquid-like T^2 law [Fig. 4(b)] highly dependent on Co concentration, which excludes an electron-phonon scattering contribution. Such electron-electron scattering processes are given by

$$\hbar/\tau_e(T) = A(k_B T)^2/E_F \quad (5)$$

where A is a dimensionless constant [22]. They are overwhelmed by phonon processes in usual metals, but are enhanced here since $k_B T \approx E_F$. For $x = 14\%$, with $E_F = 25$ meV and $m_e/m_0 = 2$ taken from ARPES, we estimate a typical value $A \approx 4$, which corroborates the validity of our analysis. We furthermore find that the T^2 coefficient displays a simple $1/n_e$ variation [inset of Fig. 4(a)], which agrees with $E_F \propto n_e^\alpha$ for a simple parabolic band, with $\alpha = 1$ in the 2D case. As for the disorder induced residual scattering rate τ_0^{-1} , we can see in Fig. 4(b) that it remains unchanged in the paramagnetic state for all x , so that native disorder dominates over the effect of Co substitution in the Fe planes.

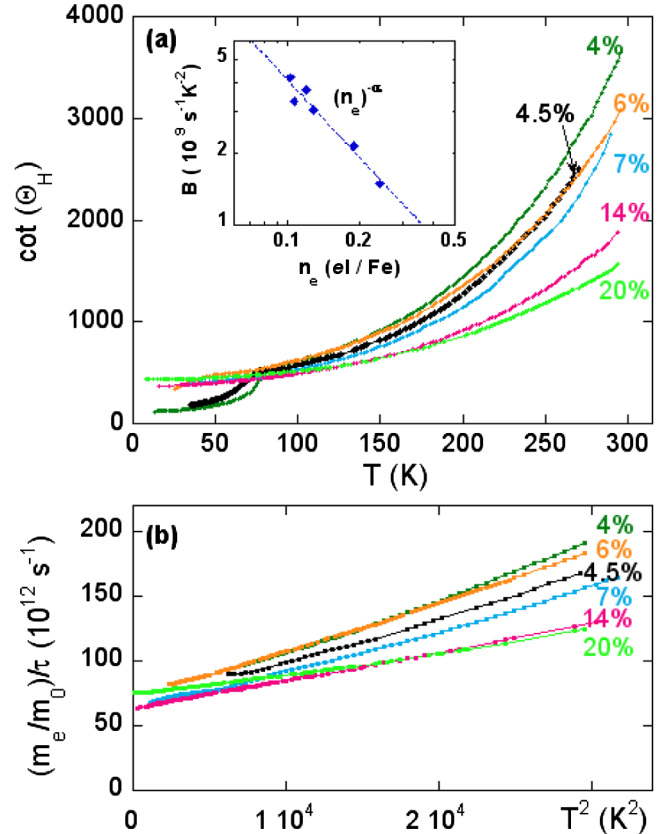


FIG. 4 (color online). (a) T variation of $\cot(\Theta_H = \rho/|R_H|)$ at 1 T. (b) This quantity, which reduces to $(m_e/m_0)/\tau$ if $\sigma_h \ll \sigma_e$, is plotted versus T^2 in the paramagnetic phase for $x \geq 4\%$. This evidences a Fermi-liquid behavior for $T \leq 150$ K. Inset: Coefficient B of the T^2 variation versus n_e in logarithmic scales. The line corresponds to $B \propto 1/n_e$.

Parent compound and weakly doped compounds.—For $x = 0$, the drop of n_H in Fig. 2 occurs in two steps: a first one at $T_{SDW} = 135$ K results in a plateau followed then by a slower decrease down to $T = 0$. Note that this two-step transition is not seen in $\rho(T)$ and that neutron scattering experiments did not reveal any modification of the magnetic order below T_{SDW} [23]. The value $|n_H| \approx 0.074$ at the plateau corresponds to half of the band calculation value $n_e = n_h = 0.15$ [6]. It matches as well the extrapolation value of $|n_H(T)|$ (triangle in Fig. 3). We notice in Fig. 2 that the remarkable parallel T variations of $|n_H|$ for $x = 0$ and 0.02 in the paramagnetic state correspond incidentally also to an abrupt loss of about 0.075 e/Fe . This ensemble of observations leads us to suggest that the first step of the SDW transition corresponds to the loss of one electronic band. This is expected from the gap opening associated with the nesting between an electron band and a hole band. The other bands appear then to undergo a gradual and less perfect nesting, as $|n_H|$ remains as low as 1.5% per Fe at low T . We can also speculate that the similar drop of $|n_H|$ for $x = 2\%$ is linked to the disappearance of one electronic band at E_F . The band structure of $BaFe_2As_2$ appears then very fragile as it is disturbed by a small shift of the chemical potential. This could be related to the strong hybridization of the electron bands near the M point of the Brillouin zone as revealed recently by ARPES measurements [8]. Further refined ARPES studies should permit to investigate these band structure modifications revealed by our results.

Discussion and conclusion.—Despite the multiband nature of the electronic structure of these pnictides we are able here to give a coherent picture of the charge transport in $Ba(Fe_{1-x}Co_x)_2As_2$ single crystals at low T . The small values of E_F in these compounds have been shown to induce unusually large variations of carrier content and of the Fermi liquid electron-electron scattering rate. The T linear contributions to $\rho(T)$ seen in the data cannot be compared with the case of single band correlated electron systems as recently proposed [11,24]. In the present multiband system the joint analysis of $\rho(T)$ and $n_H(T)$ washes out those in $1/\tau_e(T)$, which does not reflect any quantum critical behavior.

The large variations of $n_H(T)$ seen at high T imply an unexpected semiconducting-like increase of $\sigma_h(T)$. This could result from a variation of $n_e(T)$ due to a shift of the chemical potential $\mu(T)$ induced by localization of the hole carriers at low T . These variations could be related with the large high T increase of the NMR Knight shifts K [10,25] interpreted as a pseudogap, although K is not found to go through a maximum as in cuprates [16]. Others [17] suggest that the variation of $n_H(T)$ is dominated by a decrease of hole mobility due to spin fluctuations. Let us note that the critical behavior of spin fluctuations detected in NMR above T_{SDW} [10] are not directly apparent in the transport. However, we can notice that the low T carrier content is smaller than expected from band calculations up

to $x \approx 10\%$ and that the large high T increase in $|n_H(T)|$ appears mainly for the magnetic samples. In the approach of [17], this might mean that hole localization is promoted by spin fluctuations. Nevertheless, we do not understand why electron transport would not be affected as well in such a case. This unusual behavior is an originality of the electronic correlations in these compounds which requires a specific theoretical understanding.

As for SC, it seems to coexist with the SDW state in these doped compounds, contrary to the case of the electron doped 1111 family [1,26]. However, we evidence that SC only strengthens when the SDW nesting transition has been sufficiently weakened, which agrees qualitatively with the suggestion done for a ($s\pm$) superconductivity with pairing of electrons in distinct hole and electron bands [9]. Further experiments on the hole doped cases should allow to reveal any asymmetry of the phase diagram from the point of view of transport properties.

This work has been performed within the ‘‘Triangle de la Physique.’’ We thank S. Poissonnet (SRMP/CEA) for the chemical analyses of the samples. We acknowledge fruitful discussions with I. Mazin, V. Brouet, and C. Pépin. We also thank N. Kirova and P. Mendels for critical reading of the manuscript.

*florence.albenque-rullier@cea.fr

- [1] J. Zhao *et al.*, Nature Mater. **7**, 953 (2008).
- [2] H. Chen *et al.*, Europhys. Lett. **85**, 17006 (2009).
- [3] J. H. Chu *et al.*, Phys. Rev. B **79**, 014506 (2009).
- [4] D. Singh, Phys. Rev. B **78**, 094511 (2008).
- [5] I. I. Mazin and J. Schmalian, Physica C (Amsterdam) **469**, 614 (2009).
- [6] F. Ma *et al.*, arXiv:0806.3526.
- [7] D. Hsieh *et al.*, arXiv:0812.2289.
- [8] M. Yi *et al.*, arXiv:0902.2628.
- [9] I. I. Mazin *et al.*, Phys. Rev. Lett. **101**, 057003 (2008).
- [10] F. L. Ning *et al.*, J. Phys. Soc. Jpn. **78**, 013711 (2009).
- [11] M. Gooch *et al.*, Phys. Rev. B **79**, 104504 (2009).
- [12] A. Leithe-Jasper *et al.*, Phys. Rev. Lett. **101**, 207004 (2008).
- [13] A. S. Sefat *et al.*, Phys. Rev. Lett. **101**, 117004 (2008).
- [14] N. Ni *et al.*, Phys. Rev. B **78**, 214515 (2008).
- [15] X. F. Wang *et al.*, New J. Phys. **11**, 045003 (2009).
- [16] H. Alloul, J. Bobroff, M. Gabay, and P. Hirschfeld, Rev. Mod. Phys. **81**, 45 (2009).
- [17] L. Fang *et al.*, arXiv:0903.2418.
- [18] X. F. Wang *et al.*, Phys. Rev. Lett. **102**, 117005 (2009).
- [19] L. J. van der Pauw, Philips Res. Rep. **13**, 1 (1958).
- [20] Y. Sekiba *et al.*, New J. Phys. **11**, 025020 (2009).
- [21] L. X. Yang *et al.*, Phys. Rev. Lett. **102**, 107002 (2009).
- [22] N. W. Ashcroft and N. D. Mermin, *Solid State Physics* (Saunders College Publishing, Philadelphia, 1976).
- [23] S. D. Wilson *et al.*, Phys. Rev. B **79**, 184519 (2009).
- [24] N. Doiron-Leyraud *et al.*, arXiv:0905.0964.
- [25] H. J. Grafe *et al.*, New J. Phys. **11**, 035002 (2009).
- [26] H. Luetkens *et al.*, Nature Mater. **8**, 305 (2009).
- [27] D. K. Pratt *et al.*, arXiv:0903.2833.